Formation Establishment and Reconfiguration Using Impulsive Control

S. S. Vaddi*
Optimal Synthesis Inc., Palo Alto, California 94303
and
K. T. Alfriend,† S. R. Vadali,‡ and P. Sengupta§
Texas A&M University, College Station, Texas 77843-3141

We analyze spacecraft formation establishment and reconfiguration problems for two-body orbits. The desired formations are characterized by nonsingular orbital-elemental differences. An analytical, two-impulse solution is proposed for achieving the desired orbital-elemental differences. Gauss's variational equations are used to compute the corresponding impulse magnitudes analytically and the resulting solutions can be easily implemented using onboard computational resources. It is also shown that the cost obtained from the analytical solution differs by less than 1% from that obtained by numerical optimization.

Introduction

FORMATION flying is a new paradigm in space mission design, aimed at achieving the functionality of a very large satellite with multiple small satellites. The proposed benefits of formation flying include flexible mission capabilities, achieved through the reconfiguration of formations. In this paper, we address the issues of establishment and reconfiguration of spacecraft formations for two-body orbits using impulsive control. We focus our attention on formations that consist of a central chief spacecraft, surrounded by multiple deputy spacecraft. We also assume that the chief is in a circular reference orbit.

Shown in Fig. 1 is a schematic of a circular formation that will be considered in this paper. A four-deputy formation is shown in the initial(inner) configuration. Impulsive control will be used to establish a deputy at a desired position in the formation. The formation reconfiguration problem involves transferring these four deputies to four uniformly separated slots on the final configuration. Indicated on the final configuration are two different sets of slots, shown by empty circles and circles with dots at their centers. Each set consists of four uniformly separated slots in the final configuration. Though the figure shows only two such sets, it is obvious that there are infinite possibilities, and it is desired to pick the one with optimal features. The choice of the set is to be followed by the process of assigning to each deputy in the initial configuration a unique slot in the chosen set. A control strategy is also required to transfer the deputy from a given location on the initial relative orbit to any given location on the final relative orbit. The fuel consumption for the transfer process depends on the initial and final positions of the spacecraft.

Typically, impulsive control, applied at proper locations, is preferred to thrust application for an extended period. Orbital-element models offer a convenient analytical platform for designing impulsive control laws. Though the circular-orbit analysis can be conducted using Hill's state transition matrix, the orbital-element approach is more suitable for accommodating the effects of elliptic chief orbits and oblate Earth perturbation. Alfriend et al.[1,2] used a geometric approach to characterize the relative orbit in terms of orbital-element differences. Vadali et al.[3,4] used classical orbital elements to relate the constants of the Hill–Clohessy–Wiltshire periodic solutions to orbital-element differences. Schaub[5] developed a general method for describing linearized relative motion about a chief in both circular and elliptic orbits using orbital-element differences. Gauss's variational equations can be used to determine the impulse magnitudes, directions, and application times. Schaub and Alfriend[6] developed impulsive-feedback-control laws for establishing a desired set of mean-element differences. Vadali et al.[7] have also dealt with impulsive orbit-correction schemes in the presence of J_2. The works mentioned do not address the formation establishment and reconfiguration problems, but form the basis of our approach in this paper. Ahn and Spencer[8] studied the optimal reconfiguration of a formation-flying satellite constellation following the failure of a constellation member, using permutation analysis. Tillerson et al.[9] present fuel- and time-optimal control algorithms for formation reconfiguration using numerical linear and integer programming techniques, using linearized equations of relative motion dynamics. Lovell et al.[10] developed a guidance algorithm for formation reconfiguration based on the perturbed Clohessy–Wiltshire equations. Alfriend et al.[11] derived the equations for impulsive control of a satellite formation when the chief is in a low Earth orbit of small eccentricity with no radial thrusting. Irvin and Jacques[12] compared continuous and discrete burn techniques, as well as linear and nonlinear feedback control techniques for the reconfiguration of satellite formations. Gurfil[13] developed a control-theoretic framework for both analysis and design of low-thrust orbital transfers using orbital-element feedback by analyzing accessibility and stabilizability properties of Gauss equations. Wiesel[14] laid out the theoretical foundation for optimal impulse control of relative satellite motion using a Cartesian coordinate model and solved the resulting optimization problem numerically.

In this paper, we first relate the desired relative orbit periodic-solution constants to nonsingular orbital-elemental differences between the chief and deputy. Next, we develop an analytical two-impulse control scheme for transferring a deputy from a given location in the initial configuration to any given location in the final configuration, using Gauss's variational equations. An optimal solution for the pairing of each deputy with a location in the final configuration will be derived using these control schemes. It is seen that this pairing scheme not only minimizes the overall fuel consumption for the formation reconfiguration, but also results in homogeneous fuel

Presented as Paper 2003-590 at the AAS/AIAA Astrodynamics Specialist Conference, Big Sky, MT, 4–7 August 2003; received 24 November 2003; revision received 23 June 2004; accepted for publication 28 June 2004.

*Research Scientist, 868 San Antonio Road; vaddi@optisyn.com.
†TEES Research Professor and Holder of the TEES Distinguished Research Chair, Department of Aerospace Engineering; alfriend@aero.tamu.edu. Fellow AIAA.
‡Stewart & Stevenson-I Professor, Department of Aerospace Engineering; svadali@aero.tamu.edu. Associate Fellow AIAA.
§Graduate Student, Department of Aerospace Engineering; prasenjit@tamu.edu. Student Member AIAA.

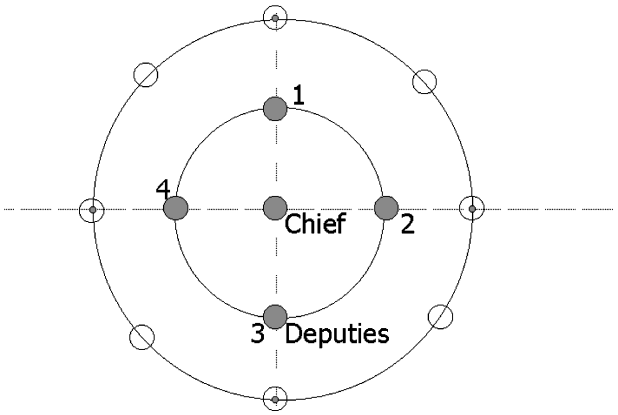

Fig. 1 Schematic diagram of a circular formation.

consumption among all the deputies. In the last section we compare the fuel consumption resulting from the analytical solution with that obtained from a numerically optimized solution.

Characterizing the Formations

The Hill–Clohessy–Wiltshire (HCW) equations[15] describe the linearized relative motion of a deputy with respect to a chief in a circular orbit around the Earth. The HCW equations admit bounded periodic solutions given by Eqs. (1–3), which are found suitable for formation flying missions. These solutions, referred to as HCW solutions, are as follows:

$$x = (c_1/2)\sin(\theta + \alpha_0) \tag{1}$$

$$y = c_1 \cos(\theta + \alpha_0) + c_3 \tag{2}$$

$$z = c_2 \sin(\theta + \alpha_0) \tag{3}$$

where x, y, and z are the relative-motion coordinates in the radial, along-track, and out-of-plane directions defined in a rotating coordinate system attached to the chief, and θ is the argument of latitude of the chief. The constants c_1, c_2, c_3, and α_0 are determined by the initial conditions:

1) Choosing $c_1 = c_2 = \rho$ and $c_3 = 0$ results in a relative orbit between the chief and the deputy that is circular when projected onto the local horizontal plane; that is, $y^2 + z^2 = \rho^2$, where ρ is a constant. This formation will be referred to as the projected circular orbit (PCO).

2) Choosing $c_1 = \rho$, $c_2 = \sqrt{3}/2\rho$, and $c_3 = 0$ results in a general circular orbit (GCO), with $x^2 + y^2 + z^2 = \rho^2$. A nonzero c_3 results in the PCO and GCO formations having a constant offset between the chief and the center of the formation.

3) Choosing $c_1 = c_2 = 0$ and $c_3 = d$, a constant, results in the leader–follower configuration. In this formation, the deputy constantly leads or trails the chief by a constant distance d in the along-track (y) direction.

We refer to ρ as the disk size in the rest of the paper. Different deputies can be initiated into the PCO and GCO formations by assigning them different values of α_0. Together, these satellites can simulate the baseline of a large circular antenna.

We now relate the constants c_1, c_2, α_0, and c_3 to orbital-element differences using an approach similar to the one adopted in Refs. 3–5 but with a different choice of orbital elements. The classical set of orbital elements given by semimajor axis a, eccentricity e, inclination i, right ascension Ω, argument of perigee ω, and mean anomaly M cannot be used for a circular orbit because the argument of perigee cannot be uniquely defined. Gauss's variational equations for ω and M also have a singularity for $e = 0$. Therefore, we choose to work with the nonsingular[16] set of orbital elements given as

$$\boldsymbol{e} = [a, q_1, q_2, i, \Omega, \lambda] \tag{4}$$

$$q_1 = e\cos\omega \tag{5}$$

$$q_2 = e\sin\omega \tag{6}$$

$$\lambda = \omega + M \tag{7}$$

It is well known from orbital mechanics that bounded relative motion between two spacecraft can be obtained only if their periods are equal. This in turn requires that their semimajor axes be the same or their difference δa be zero. All of the orbital elements other than λ are constant for each spacecraft and hence their differences are also constant. However, with $\delta a = 0$, we also have $\delta\lambda = \text{constant}$, which makes it a suitable choice to relate to the periodic solution constants.

From the geometric description[1] of linearized relative motion we have

$$y = a(\delta\theta + \delta\Omega\cos i) \tag{8}$$

$$z = a(\delta i\sin\theta - \delta\Omega\cos\theta\sin i) \tag{9}$$

These equations describe the relative motion between a spacecraft in a circular reference orbit with semimajor axis a, inclination i, and latitude angle described by θ, and any nearby spacecraft with orbital-elemental differences given by $[\delta\theta \;\; \delta i \;\; \delta\Omega]$. The argument of latitude θ is defined as

$$\theta = \omega + f \tag{10}$$

$$\Rightarrow \delta\theta = \delta\omega + \delta f \tag{11}$$

The true anomaly f can be approximated as follows for a near-circular orbit[16]:

$$f \approx M + 2e\sin M \tag{12}$$

$$\Rightarrow \theta \approx \lambda + 2q_1\sin\lambda - 2q_2\cos\lambda \tag{13}$$

Though the eccentricity of the chief is assumed to be zero, we retain it in the series expansion for f because δe is not necessarily equal to 0. Therefore, the variation in the latitude for a circular reference orbit($q_1 = q_2 = 0$) can be written as follows:

$$\delta\theta \approx \delta\lambda + 2\delta q_1\sin\lambda - 2\delta q_2\cos\lambda \tag{14}$$

Grouping the constant terms and harmonic terms, separately, the along-track (y) equation can be written as follows:

$$y = a[\delta\lambda + \delta\Omega\cos i] + \sin\lambda[2a\delta q_1] + \cos\lambda[-2a\delta q_2] \tag{15}$$

For a circular reference orbit, $\theta = \lambda$. Therefore, the relation for z can also be rewritten in terms of orbital-elemental differences as follows:

$$z = a(\delta i\sin\lambda - \delta\Omega\cos\lambda\sin i) \tag{16}$$

The desired periodic solution for y and z given by Eqs. (2) and (3) can be expanded as follows:

$$y = c_3 + c_1\cos\lambda\cos\alpha_0 - c_1\sin\lambda\sin\alpha_0 \tag{17}$$

$$z = c_2\sin\lambda\cos\alpha_0 + c_2\cos\lambda\sin\alpha_0 \tag{18}$$

In this paper we focus on the PCO and GCO formations; therefore we set $c_3 = 0$. Comparing coefficients of $\cos\lambda$ and $\sin\lambda$ in Eqs. (17) and (18) with those in Eqs. (15) and (16), respectively, we obtain the following set of orbital-elemental differences to generate the desired HCW periodic solutions:

$$\delta a = 0 \tag{19}$$

$$\delta q_1 = -\frac{c_1\sin\alpha_0}{2a} \tag{20}$$

$$\delta q_2 = -\frac{c_1\cos\alpha_0}{2a} \tag{21}$$

$$\delta i = \frac{c_2 \cos\alpha_0}{a} \tag{22}$$

$$\delta\Omega = -\frac{c_2 \sin\alpha_0}{a \sin i} \tag{23}$$

$$\delta\lambda = -\delta\Omega \cos i \tag{24}$$

Impulsive Control

In the preceding section, we prescribed the required set of elemental differences to establish the desired HCW formations. In this section we employ Gauss's variational equations[16] in establishing these elemental differences using impulsive thrust. Gauss' variational equations in terms of nonsingular elements, for a circular reference orbit, can be written as follows:

$$\delta i \approx \gamma \cos\theta \Delta V_h \tag{25}$$

$$\delta\Omega \approx (\gamma \sin\theta / \sin i)\Delta V_h \tag{26}$$

$$\delta a \approx (2/n)\Delta V_t \tag{27}$$

$$\delta q_1 \approx \gamma \sin\theta \Delta V_r + 2\gamma \cos\theta \Delta V_t \tag{28}$$

$$\delta q_2 \approx -\gamma \cos\theta \Delta V_r + 2\gamma \sin\theta \Delta V_t \tag{29}$$

$$\delta\lambda \approx -2\gamma \Delta V_r - \gamma \sin\theta \cot i \Delta V_h \tag{30}$$

where $\gamma = \sqrt{a/\mu}$. ΔV_r, ΔV_t, and ΔV_h are the magnitudes of the impulse components in the radial, tangential, and out-of-plane directions, respectively. Even though the deputy is in a slightly elliptic orbit, Gauss's variational equations for a circular orbit were used because higher order terms such as the products of the elemental differences and the products of elemental differences and impulse magnitudes (assuming small controls) were neglected in the derivation of these equations.

In this paper, we assume that there are three different thrusters, one for each direction. The fuel consumption due to a single impulse is proportional to the one norm of the impulse vector:

$$\text{FC} \propto |\Delta V_r| + |\Delta V_t| + |\Delta V_h| \tag{31}$$

Formationwide fuel consumption can be related to the summation of the absolute values of the impulse components over the total number of impulses and total number of spacecraft in the formation. It should be noted that the fuel consumption metric for a single-thruster spacecraft would be proportional to the two-norm of the impulse vector.

It can be seen from Eqs. (25) and (26) that the inclination and the node are affected by the out-of-plane thrust alone. In this paper, the out-of-plane cost refers to the cost of creating the desired inclination and the desired nodal differences. The in-plane cost refers to the cost of creating the remaining four elemental differences. It should be noted that other than λ, the remaining three elemental differences are affected by the radial and tangential thrust alone. In the following section, we consider the establishment of the out-of-plane elemental differences.

Establishment of Out-of-Plane Elemental Differences

The desired inclination difference and the node difference can be obtained by one impulse, suitably located at the following latitude angle:

$$\theta_o = \tan^{-1}\left(\frac{\delta\Omega \sin i}{\delta i}\right) \tag{32}$$

This equation has two solutions separated by 180 deg and either of them can be chosen. The ΔV_h corresponding to the two θ_o locations is given next:

$$\Delta V_h = \pm(1/\gamma)\sqrt{\delta i^2 + \delta\Omega^2 \sin^2 i} \tag{33}$$

Desirable Side Effect

The out-of-plane impulse ΔV_h given by Eq. (33) also creates a $\delta\lambda$, given by

$$\delta\lambda = -\frac{r \sin\theta \cos i}{h \sin i}\Delta V_h = -\delta\Omega \cos i \tag{34}$$

The desired $\delta\lambda$ for zero bias formation is given by Eq. (24) and is exactly the same as $-\delta\Omega \cos i$. Therefore, the out-of-plane impulse given by Eq. (33) not only establishes the out-of-plane elemental differences, but also establishes the desired $\delta\lambda$ for the PCO and GCO formations.

Aside

The out-of-plane impulse can also be split up into two components at two locations θ_o and $\theta_o + \pi$:

$$\Delta V_{h_1} = \pm(p/\gamma)\sqrt{\delta i^2 + \delta\Omega^2 \sin^2 i} \tag{35}$$

$$\Delta V_{h_2} = \pm[(1-p)/\gamma]\sqrt{\delta i^2 + \delta\Omega^2 \sin^2 i} \tag{36}$$

where $p \in [0\ \ 1]$. Splitting the out-of-plane into two components does not change fuel consumption of a three-thruster spacecraft because $|\Delta V_{h_1}| + |\Delta V_{h_2}| = |\Delta V_h|$ for all choices of p. However, the choice of p can influence the fuel consumption of a single thruster spacecraft.

Establishment of In-Plane Elemental Differences

In this section, we address the establishment of in-plane elemental differences using radial and tangential thrusting only. The impulse equations for the in-plane elemental differences are given by Eqs. (27–30). At least two impulses are required to establish the four elemental differences. It was observed from numerical experiments that the optimal angular separation between the two impulses is 180 deg. Therefore, we choose the latitude angles of the impulse locations to be θ and $\theta + \pi$. With this assumption, we now analyze the impulse equations for the in-plane elemental differences. We first look at the δa equation, which is independent of θ:

$$\delta a = (2/n)\Delta V_{t_1} + (2/n)\Delta V_{t_2} \tag{37}$$

The subscripts 1 and 2 refer to the first and second impulses. The desired δa is equal to 0; therefore the two tangential impulse components have to be equal and opposite to each other:

$$\Rightarrow \Delta V_{t_1} = -\Delta V_{t_2} = \Delta V_t \tag{38}$$

The equations for δq_1 and δq_2 can similarly be written as follows:

$$\begin{aligned}\delta q_1 &= \gamma\left[\sin\theta \Delta V_{r_1} + 2\cos\theta \Delta V_{t_1}\right] \\ &\quad + \gamma\left[\sin(\theta+\pi)\Delta V_{r_2} + 2\cos(\theta+\pi)\Delta V_{t_2}\right] \\ &= \gamma\left[\sin\theta \Delta V_{r_1} + 4\cos\theta \Delta V_t - \sin\theta \Delta V_{r_2}\right]\end{aligned} \tag{39}$$

$$\begin{aligned}\delta q_2 &= \gamma\left[-\cos\theta \Delta V_{r_1} + 2\sin\theta \Delta V_{t_1}\right] \\ &\quad + \gamma\left[-\cos(\theta+\pi)\Delta V_{r_2} + 2\sin(\theta+\pi)\Delta V_{t_2}\right] \\ &= \gamma\left[-\cos\theta \Delta V_{r_1} + 4\sin\theta \Delta V_t + \cos\theta \Delta V_{r_2}\right]\end{aligned} \tag{40}$$

The equation for $\delta\lambda$ is as follows:

$$\delta\lambda = \delta n_1(t_2 - t_1) - 2\gamma \Delta V_{r_1} - 2\gamma \Delta V_{r_2} = 0 \tag{41}$$

Though the task of creating the desired $\delta\lambda = -\cos i\,\delta\Omega$ has been achieved by the out-of-plane impulse, another side effect resulting from the two tangential impulses needs to be corrected, as shown by Eq. (41). The term $\delta n_1(t_2 - t_1)$ is the drift that occurs due to the change in the semimajor axis that is created by the first tangential impulse. The times t_1 and t_2 are, respectively, the times of application

of the first and second impulse. At the end of the second impulse, δa will be equal to zero and hence δn will also be equal to zero. Once, $\delta n = 0$ is established, $\delta\lambda$ remains a constant. δn_1 can be related to the first tangential impulse component as follows:

$$n = \sqrt{\mu/a^3} \tag{42}$$

$$\delta n_1 = (-3n/2a)\delta a_1 \tag{43}$$

where δa_1 is the semimajor axis difference that is created after the first impulse, which can be written as

$$\delta a_1 = (2/n)\Delta V_{t_1} \tag{44}$$

The impulse application times t_1 and t_2, are separated by one half period, due to the choice of 180 deg spacing between the impulses. Hence $t_2 - t_1 = T_p/2 = \pi/n$, where n is the mean motion and T_p is the time period of the chief's orbit. Therefore, the drift due to the change in semimajor axis resulting form the first impulse can be written as follows:

$$\delta n_1(t_2 - t_1) = (-3\pi/an)\Delta V_t \tag{45}$$

Finally, Eq. (41) reduces to the following:

$$\delta\lambda = -2\gamma\Delta V_{r_1} - 2\gamma\Delta V_{r_2} - (3\pi/an)\Delta V_t = 0 \tag{46}$$

ΔV_{r_1}, ΔV_{r_2}, and ΔV_t are obtained by solving the three equations (39), (40), and (46):

$$\Delta V_t = \Delta V_{t_1} = \frac{\delta q_1 \cos\theta + \delta q_2 \sin\theta}{4\gamma} = -\Delta V_{t_2} \tag{47}$$

$$\Delta V_{r_1} = \frac{\delta q_1 \sin\theta - \delta q_2 \cos\theta}{2\gamma} - \frac{3\pi}{an}\frac{\delta q_1 \cos\theta + \delta q_2 \sin\theta}{16\gamma^2} \tag{48}$$

$$\Delta V_{r_2} = -\frac{\delta q_1 \sin\theta - \delta q_2 \cos\theta}{2\gamma} - \frac{3\pi}{an}\frac{\delta q_1 \cos\theta + \delta q_2 \sin\theta}{16\gamma^2} \tag{49}$$

These equations can further be simplified as follows:

$$\Delta V_t = \frac{\sqrt{\delta q_1^2 + \delta q_2^2}}{4\gamma}\sin(\theta + \xi) \tag{50}$$

where ξ is an angle given by $\xi = \tan^{-1}(\delta q_1/\delta q_2)$:

$$\Delta V_{r_1} = -\frac{\sqrt{\delta q_1^2 + \delta q_2^2}}{2\gamma}\left[\cos(\theta + \xi) + \frac{3\pi}{8an\gamma}\sin(\theta + \xi)\right] \tag{51}$$

This equation can be simplified by recognizing that the term $an\gamma$ is equal to 1:

$$\Rightarrow \Delta V_{r_1} = -\frac{\sqrt{\delta q_1^2 + \delta q_2^2}}{2\gamma}\frac{\sqrt{64 + 9\pi^2}}{8}\sin(\theta + \xi + \psi) \tag{52}$$

where ψ is another constant angle given by $\psi = \tan^{-1}[1/3\pi/8)]$. Similarly, the equations for ΔV_{r_2} can also be written as follows:

$$\Delta V_{r_2} = -\frac{\sqrt{\delta q_1^2 + \delta q_2^2}}{2\gamma}\frac{\sqrt{64 + 9\pi^2}}{8}\sin(\theta + \xi - \psi) \tag{53}$$

We now consider optimizing the following function with respect to θ:

$$\begin{aligned}\Delta V_i &= \left|\Delta V_{r_1}\right| + \left|\Delta V_{t_1}\right| + \left|\Delta V_{r_2}\right| + \left|\Delta V_{t_2}\right| \\ &= \left|\Delta V_{r_1}\right| + 2\left|\Delta V_t\right| + \left|\Delta V_{r_2}\right|\end{aligned} \tag{54}$$

The subscript i refers to in-plane cost, in contrast to the out-of-plane cost obtained in the preceding section. Substituting Eqs. (50–53) into the equations, we obtain the following:

$$\Delta V_i(\theta) = \frac{\sqrt{\delta q_1^2 + \delta q_2^2}}{2\gamma}\left[|\sin(\theta + \xi)| + \sqrt{1 + \frac{9\pi^2}{64}}\{|\sin(\theta + \xi - \psi)| + |\sin(\theta + \xi + \psi)|\}\right] \tag{55}$$

This function is nondifferentiable at the following points:

$$\theta = \pi - \xi, \quad 2\pi - \xi, \quad \pi - \xi - \psi, \quad 2\pi - \xi - \psi, \quad \pi - \xi + \psi, \quad 2\pi - \xi + \psi \tag{56}$$

We now prove that the minimum value of $\Delta V(\theta)$ given by Eq. (55) occurs at one of these nondifferentiable points. The proof is given below for a more general problem on the same lines.

Lemma: The minimum value of the function

$$J(\theta) = \sum_{j=1}^{k} |A_j \sin(\theta + \chi_j)|$$

where A_j's(>0) are the constant amplitudes and χ_j's$(\in [0\ 2\pi])$ are the constant phase angles, occurs at a point $\theta = \theta_i$ where the function is not differentiable.

Proof: We adopt a proof by contradiction approach. We prove that the function cannot have a minimum value at a point $\theta = \theta^*$, where the function $J(\theta)$ is differentiable. The function $J(\theta)$ is periodic with a period of 2π; therefore we focus our attention in the interval $\theta \in [0\ 2\pi]$. $J(\theta)$ is also nondifferentiable at the points $\theta = \pi - \chi_j$ and $\theta = 2\pi - \chi_j$, $j \in [1, k]$. However, the function is differentiable at all points between any two consecutive nondifferentiable points. Moreover, the function can be written as a single sinusoidal function $J(\theta) = A\sin(\theta + \chi)$ in each of these segments. The constants $A(>0)$ and χ can be obtained as functions of A_j and χ_j in each segment, differently. For a minimum value to occur at a point $\theta = \theta_i$ that lies in these segments, the following conditions need to be satisfied:

$$\left.\frac{\partial J(\theta)}{\partial\theta}\right|_{\theta=\theta_i} = -A\cos(\theta + \chi)|_{\theta=\theta_i} = 0 \tag{57}$$

$$\left.\frac{\partial^2 J(\theta)}{\partial\theta^2}\right|_{\theta=\theta_i} = -A\sin(\theta + \chi)|_{\theta=\theta_i} = -AJ(\theta)|_{\theta=\theta_i} > 0 \tag{58}$$

The function $J(\theta) > 0$ for all values of θ and the constant A is also greater than zero which implies $-AJ(\theta)$ is always less than zero. Therefore, Eq. (58) can never be satisfied by the function $J(\theta)$; hence, it cannot have a minimum value at a point $\theta = \theta_i$ where the function is differentiable. Therefore, the minimum value has to occur at a nondifferentiable point.

Per the preceding lemma, the minimum value of $\Delta V_i(\theta)$ given by Eq. (55) occurs at one of the six values of θ, given by Eq. (56). The search further reduces to two evaluations due to the following:

$$\Delta V_i(\pi - \xi) = \Delta V_i(2\pi - \xi) = \sqrt{\left(\delta q_1^2 + \delta q_2^2\right)}\Big/\gamma \tag{59}$$

$$\begin{aligned}\Delta V_i(\pi - \xi - \psi) &= \Delta V(2\pi - \xi - \psi) = \Delta V_i(\pi - \xi + \psi) \\ &= \Delta V(2\pi - \xi + \psi) = 1.0859\sqrt{\left(\delta q_1^2 + \delta q_2^2\right)}\Big/\gamma\end{aligned} \tag{60}$$

Therefore, the optimal θ locations for establishment of in-plane elemental differences are $\pi - \xi$, $2\pi - \xi$. It should be noted that they are separated by 180 deg. Therefore, making either of the two choices above for the first impulse only results in the second impulse location being the other choice. In this paper, we choose $2\pi - \xi$ as the location for the first impulse. It is interesting to note that the tangential components of the two-impulse solution are identically

Table 1 Impulse components and locations for a two-impulse scheme

Component	First impulse	Second impulse
Location	$\theta = \theta_o$	$\theta = \theta_o + \pi$
Radial	$-\dfrac{\sqrt{\delta q_1^2 + \delta q_2^2}}{2\gamma}$	$\dfrac{\sqrt{\delta q_1^2 + \delta q_2^2}}{2\gamma}$
Tangential	0	0
Out-of-plane	$\dfrac{\sqrt{\delta i^2 + \delta\Omega^2 \sin^2 i}}{\gamma}$	0

equal to zero at $\theta = 2\pi - \xi$. This can easily be verified by substituting $\theta = 2\pi - \xi$ into Eq. (50). The absence of tangential thrust also eliminates the λ drift resulting from the first tangential impulse. The radial components of the first and second impulses are obtained by substituting $\theta = 2\pi - \xi$ into Eqs. (48) and (49). The resulting impulse components are equal and opposite to each other:

$$\Delta V_{r_1} = -\Delta V_{r_2} = -\sqrt{\left(\delta q_1^2 + \delta q_2^2\right)}\Big/2\gamma \tag{61}$$

Therefore, the optimal in-plane cost is given by the following equation:

$$\Delta V_i = |\Delta V_{r_1}| + |\Delta V_{r_2}| = \sqrt{\left(\delta q_1^2 + \delta q_2^2\right)}\Big/\gamma \tag{62}$$

Formation Establishment

The formation establishment problem involves introducing a deputy into the formation with the desired element differences given by Eqs. (19–24) with respect to the chief. The optimal location for establishing the out-of-plane element differences and $\delta\lambda$ is given by Eq. (32). Substituting $\delta\Omega$ and δi from Eqs. (22) and (23) into Eq. (32), we obtain the following:

$$\theta_o = \tan^{-1}\left(\frac{-c_2 \sin\alpha_0}{c_2 \cos\alpha_0}\right) = 2\pi - \alpha_0 \tag{63}$$

The location of the first in-plane establishment impulse was found to be $\theta_i = 2\pi - \xi$. The angle $\xi = \tan^{-1}(\delta q_1/\delta q_2)$. Substituting Eqs. (20) and (21) in to this Eq. (63), we obtain the following:

$$\xi = \tan^{-1}\left(\frac{c_1 \sin\alpha_0}{c_1 \cos\alpha_0}\right) = \alpha_0 \tag{64}$$

$$\Rightarrow \theta_i = 2\pi - \xi = 2\pi - \alpha_0 = \theta_o \tag{65}$$

Therefore, the optimal location for establishing the out-of-plane impulse differences is the same as the optimal location of the first impulse for establishing the in-plane elemental differences. This implies that only two impulses are required to establish the elemental differences corresponding to the HCW formations. The impulse magnitudes are computed per Table 1. It should be noted that the total magnitude of the radial components is only half that of the out-of-plane component.

The following orbital elements of the chief are used in all of the simulations: $a = 7100$ km, $q_1 = q_2 = 0$, $i = 70$ deg, $\Omega = 10$ deg, and $\lambda = 30$ deg. The relative orbits established with the two-impulse scheme are shown in Figs. 2 (for the $\alpha = 60$ deg deputy and disk size $\rho = 1$ km) and 3 (for the $\alpha = 45$ deg deputy and disk size $\rho = 1$ km). The chief and the deputy are assumed to be coincident initially. Hence, the relative orbit starts from the origin.

Reconfiguration

In the preceding section, we used the two-impulse scheme for establishing the projected and general circular relative orbits for different deputies in a formation. In this section, we will study the reconfiguration problem, which involves changing the radius of the circular orbits from ρ_i to ρ_f. The subscripts i and f stand for initial and final, respectively. The reconfiguration problem involves two subproblems: 1) the problem of transferring the satellite from a given location on the initial relative orbit to a given location on the final relative orbit and 2) the problem of assigning, for each satellite on the initial relative orbit, the optimal location on the final relative orbit.

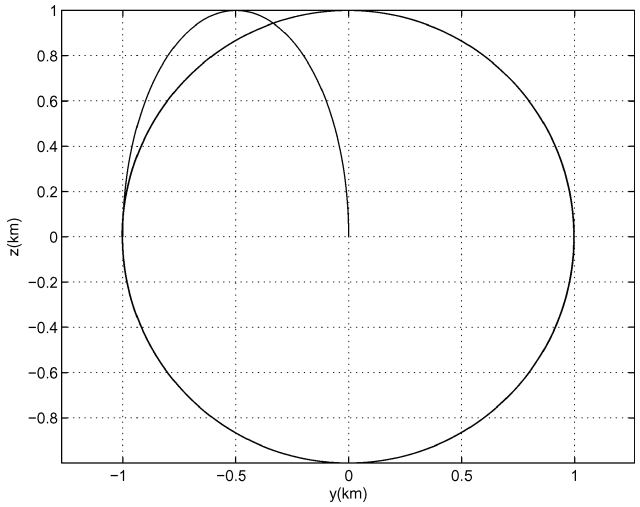

Fig. 2 Projected circular orbit established with the two-impulse solution.

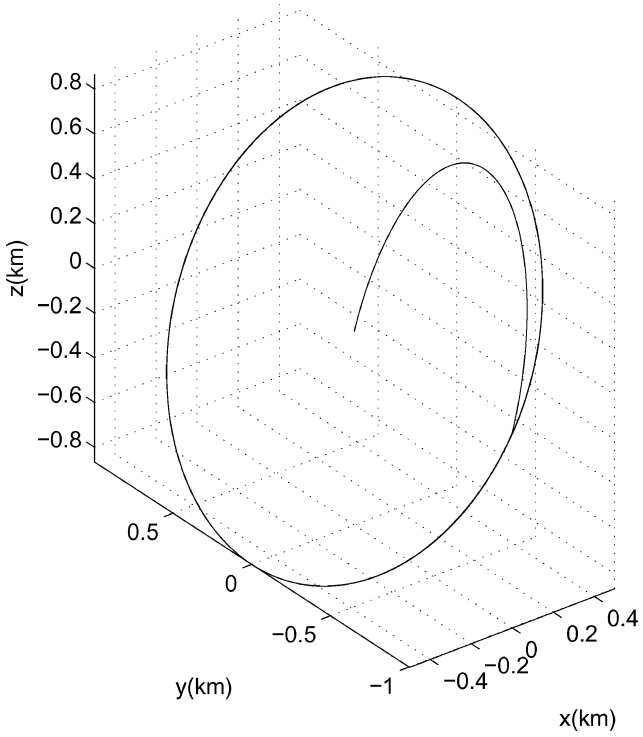

Fig. 3 General circular orbit established with the two-impulse solution.

The first problem can be solved by the two-impulse analytical solution derived in the preceding section. The desired elemental differences are computed by Eqs. (66–71):

$$\delta a = 0 \tag{66}$$

$$\delta q_1 = -\frac{c_{1_f}}{2a}\sin\alpha_{0_f} + \frac{c_{1_i}}{2a}\sin\alpha_{0_i} \tag{67}$$

$$\delta q_2 = -\frac{c_{1_f}}{2a}\cos\alpha_{0_f} + \frac{c_{1_i}}{2a}\cos\alpha_{0_i} \tag{68}$$

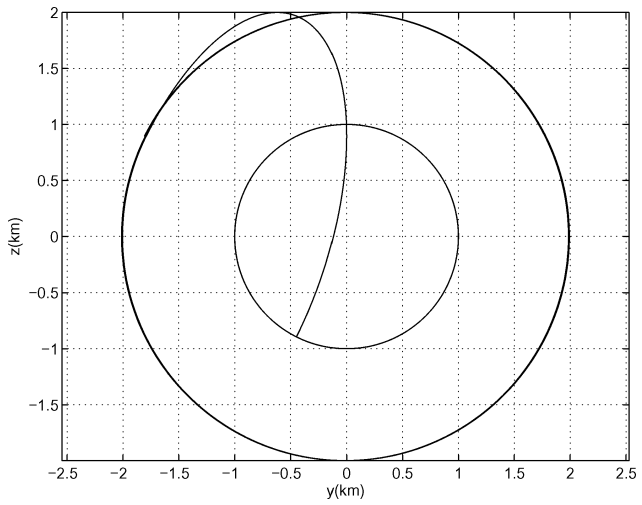

Fig. 4 Transferring the $\alpha_{0_i} = 0$ deg deputy on the PCO disk $\rho_i = 1$ km to $\alpha_{0_f} = 90$ deg on the PCO disk $\rho_f = 2$ km.

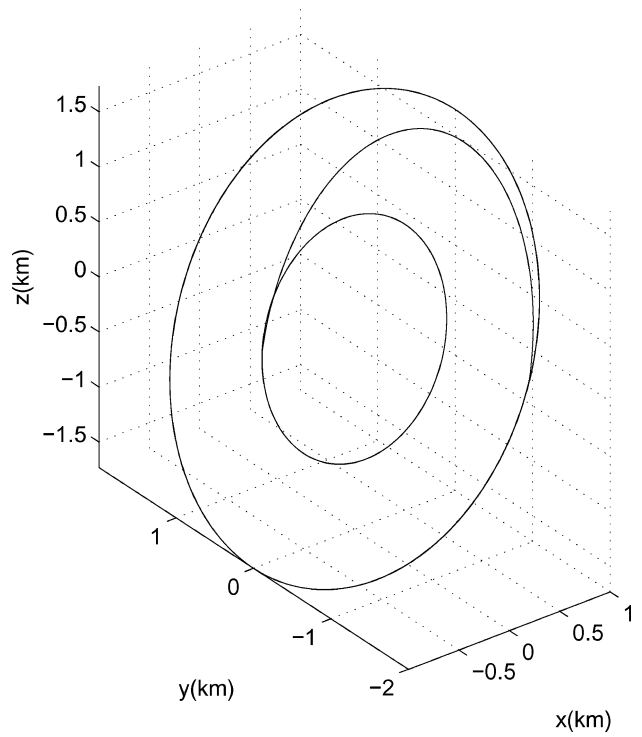

Fig. 5 Transferring the $\alpha_{0_i} = 45$ deg deputy on the GCO disk $\rho_i = 1$ km to $\alpha_{0_f} = 60$ deg on the GCO disk $\rho_f = 2$ km.

$$\delta i = \frac{c_{2_f}}{a}\cos\alpha_{0_f} - \frac{c_{2_i}}{a}\cos\alpha_{0_i} \tag{69}$$

$$\delta\Omega = \frac{c_{2_f}}{a}\frac{\sin\alpha_{0_f}}{\sin i} - \frac{c_{2_i}}{a}\frac{\sin\alpha_{0_i}}{\sin i} \tag{70}$$

$$\delta\lambda = \delta\lambda_f - \delta\lambda_i = -\delta\Omega_f\cos i + \delta\Omega_i\cos i = -\delta\Omega\cos i \tag{71}$$

where α_{0_i} and α_{0_f}, are the phase angles of the deputy on the initial and final relative orbits, respectively. Figures 4 and 5 show two instances of the transfer problem, accomplished using the two-impulse scheme. It should be noted that both the scenarios involve changing the disk size as well as α_0. The control scheme can also be used to change α_0 alone without changing the disk size after the corresponding elemental differences are computed.

The satellite slot assignment problem involves assigning, for each deputy characterized by α_{0_i} on the initial relative orbit, a unique α_{0_f} on the final relative orbit. Because there are infinite assignment possibilities, a unique solution will be obtained by minimizing the formationwide fuel consumption. Assuming there are k satellites in the initial relative orbit, k slots are required in the final relative orbit, for a unique pairing. The overall fuel consumption is proportional to

$$\sum_{l=1}^{k}\Delta V_l$$

where ΔV for each deputy is governed by α_{0_i} and the choice of α_{0_f} and is given by the following expression:

$$\Delta V\left(\alpha_{0_i}, \alpha_{0_f}\right) = \left|\Delta V_h\left(\alpha_{0_i}, \alpha_{0_f}\right)\right| + \left|\Delta V_i\left(\alpha_{0_i}, \alpha_{0_f}\right)\right| \tag{72}$$

Substituting Eqs. (33) and (62) into Eq. (72) we obtain the following:

$$\Delta V\left(\alpha_{0_i}, \alpha_{0_f}\right) = \sqrt{(\delta i^2 + \delta\Omega^2\sin^2 i)}/\gamma + \sqrt{\left(\delta q_1^2 + \delta q_2^2\right)}/\gamma \tag{73}$$

Substituting the expressions for the elemental differences given by Eqs. (67) to (70) into these equations, we obtain the following:

$$\Delta V\left(\alpha_{0_i}, \alpha_{0_f}\right) = \frac{\sqrt{c_{2_i}^2 + c_{2_f}^2 - 2c_{2i}c_{2f}\cos\left(\alpha_{0_i} - \alpha_{0_f}\right)}}{a\gamma} + \frac{\sqrt{c_{1_i}^2 + c_{1_f}^2 - 2c_{1i}c_{1f}\cos\left(\alpha_{0_i} - \alpha_{0_f}\right)}}{2a\gamma} \tag{74}$$

Clearly, this expression attains its minimum value at $\alpha_{0_i} = \alpha_{0_f}$. This indicates that each satellite has a unique minimum-fuel transfer target slot. Pairing each individual satellite with its minimum-fuel slot also minimizes the overall fuel consumption. Therefore, the optimal pairing assignment is $\alpha_{0_i} = \alpha_{0_f}$. Also, the minimum value is given by

$$\Delta V = \frac{|(c_{2f} - c_{2i})|}{\gamma a} + \frac{|(c_{1f} - c_{1i})|}{2\gamma a} \tag{75}$$

It should be noted that this expression is independent of α_{0_i} and α_{0_f}. Hence different satellites with different values of α_{0_i} consume the same fuel to reach their optimal target slots, $\alpha_{0_f} = \alpha_{0_i}$. Therefore, the two-impulse analytical solution results in homogeneous fuel consumption for different satellites in the formation during the reconfiguration maneuver.

Comparison with Numerical Results

In this section, we compare the analytical solution with results obtained using NPOPT,[17] a numerical nonlinear optimization tool. The formation reconfiguration problem has been posed as a two-impulse optimization problem as follows:

Cost function	$\|\Delta V_{r_1}\| + \|\Delta V_{t_1}\| + \|\Delta V_{h_1}\| + \|\Delta V_{r_2}\| + \|\Delta V_{t_2}\| + \|\Delta V_{h_2}\|$
Optimization variables	$\Delta V_{r_1}, \Delta V_{t_1}, \Delta V_{h_1}, \Delta V_{r_2}, \Delta V_{t_2}, \Delta V_{h_2}, \theta_1, \theta_2$
Constraints	Establishment of Eqs. (66–71)
Model	Gauss's variational equations, used for constraint evaluation

Shown in Fig. 6 is a comparison of the analytical scheme cost(continuous line) with the numerical cost(+ marks), for a two-impulse PCO reconfiguration maneuver from $\rho_i = 1$ km to $\rho_f = 2$ km. Two plots have been shown, one for the $\alpha_{0_i} = 0$ deg satellite and the other for the $\alpha_{0_i} = 90$ deg satellite. Plotted along the x-axis is the target α_0 and plotted along the y axis is the cost for transferring the 0- and 90-deg satellites to the target α_0. An all-zero initial guess was used to obtain the optimal solution for transferring the $\alpha_0 = 0$ deg satellite to the $\alpha_0 = 0$ deg slot. The solution thus obtained is used as an initial guess for the transfer to $\alpha_0 = 10$ deg and the process is repeated to obtain solutions till 90 deg. The cost resulting from the analytical scheme is found to differ from the cost resulting from numerical optimization by less than 1%. The angular separation between the impulses was also found to differ from 180 deg by less than 1 deg for this PCO reconfiguration example.

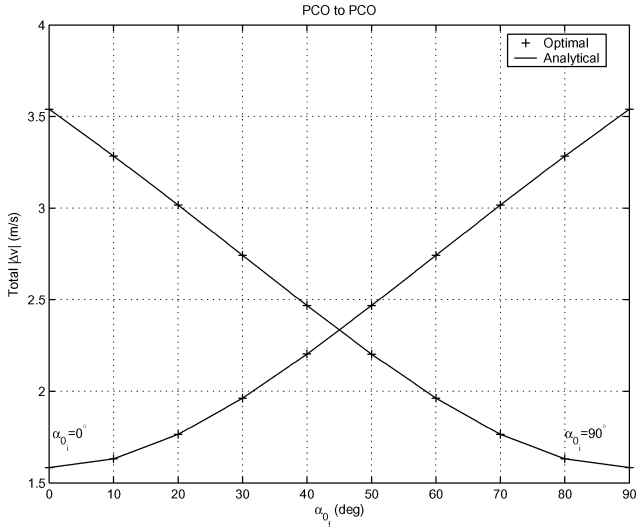

Fig. 6 Analytical control cost and optimized control cost for a PCO reconfiguration.

Conclusions

Hill–Clohessy–Wiltshire formations are characterized in terms of nonsingular orbital element differences. A two-impulse analytical solution has been developed for the formation establishment and reconfiguration problems. The analytical scheme not only provides a fuel-optimal solution to the assignment problem, but also results in homogeneous fuel consumption for different satellites in a formation. Moreover, the results are found to match very closely with similar results obtained by numerical optimization.

Acknowledgments

This research was supported by NASA Grant NAG-11349. The authors thank Dong-Woo Gim at Texas A&M University for sharing his knowledge of nonsingular elements. Thanks are also due to Darbha Swaroop at Texas A&M University for inputs on nondifferentiable optimization.

References

[1]Alfriend, K. T., Schaub, H., and Gim, D. W., "Gravitational Perturbations, Nonlinearity and Circular Orbit Assumption Effects on Formation Flying Control Strategies," 23rd Annual AAS Guidance and Control Conf., AAS Paper 00-012, Feb. 2000.

[2]Alfriend, K. T., Gim, D. W., and Vadali, S. R., "The Characterization of Formation Flying Satellite Relative Motion Orbits," AAS/AIAA Space Flight Mechanics Meeting, AAS Paper 02-143, Jan. 2002.

[3]Vadali, S. R., Vaddi, S. S., and Alfriend, K. T., "A New Concept for Controlling Formation Flying Satellite Constellations," AAS/AIAA Space Flight Mechanics Meeting, AAS Paper 01-218, Feb. 2001.

[4]Vadali, S. R., Vaddi, S. S., Naik, K. S., and Alfriend, K. T., "Control of Satellite Formations," AIAA Paper 2001-4028, July–Aug. 2001.

[5]Schaub, H., "Relative Orbit Geometry Through Classical Orbit Element Differences," *Journal of Guidance, Control, and Dynamics*, Vol. 27, No. 5, 2004, pp. 839–848.

[6]Schaub, H., and Alfriend, K. T., "Impulsive Feedback Control to Establish Specific Mean Orbit Elements of Spacecraft Formations," *Journal of Guidance, Control, and Dynamics*, Vol. 24, No. 4, 2001, pp. 739–745.

[7]Vadali, S. R., Schaub, H., and Alfriend, K. T., "Initial Conditions and Fuel Optimal Control for Formation Flying of Satellites," AIAA Guidance, Navigation, and Control Conf., July–Aug. 1999.

[8]Ahn, Y. T., and Spencer, D. B., "Optimal Reconfiguration of a Formation Flying Satellite Constellation," 53 International Astronautical Congress: The World Space Congress—2002, Oct. 2002.

[9]Tillerson, M., Inalhan, G., and How, J. P., "Co-Ordination and Control of Distributed Spacecraft Systems Using Convex Optimization Techniques," *International Journal of Robust and Nonlinear Control*, Vol. 12, No. 2, 2002, pp. 207–242.

[10]Lovell, T. A., Tragesser, S. G., Tollefson, M. V., and Horneman, K. R., "A Guidance Algorithm for Formation Reconfiguration and Maintenance Based on the Perturbed Clohessy–Wiltshire Equations," AAS/AIAA Astrodynamics Specialist Con., AAS Paper 03-649, Aug. 2003.

[11]Alfriend, K. T., Vaddi, S. S., and Lovell, T. A., "Formation Maintenance For Low Earth Near-Circular Orbits," AAS/AIAA Astrodynamics Specialist Conf., AAS Paper 03-652, Aug. 2003.

[12]Irvin, D. J., and Jacques, D. R., "Linear vs. Nonlinear Control Techniques for the Reconfiguration of Satellite Formations," AIAA Paper 2001-4089, Aug. 2001.

[13]Gurfil, P., "Control-Theoretic Analysis of Low-Thrust Orbital Transfer Using Orbital Elements," *Journal of Guidance, Control, and Dynamics*, Vol. 26, No. 6, 2003, pp. 97–115.

[14]Wiesel, W. E., "Optimal Impulse Control of Relative Satellite Motion," *Journal of Guidance, Control, and Dynamics*, Vol. 26, No. 1, 2003, pp. 74–78.

[15]Prussing, J. E., and Conway, B. A., *Orbital Mechanics*, Oxford Univ. Press, New York, 1996, pp. 143–147.

[16]Battin, R. H., *An Introduction to the Mathematics and Methods of Astrodynamics*, AIAA, Reston, VA, 1999, pp. 200, 490–494.

[17]Gill, P. E., Murray, W., and Saunders, M. A., *Users Guide for SNOPT Version 6, A FORTRAN Package for Large-Scale Nonlinear Programming*, Dept. of Mathematics, Univ. of California, La Jolla, CA/Systems Optimization Lab., Stanford Univ., Stanford, CA, 2002.